Holder et al., 2018, LinT, a simplified approach to oxygen-isotope thermometry and speedometry of high-grade rocks: An example from ultrahigh-temperature gneisses of southern Madagascar: Geology, https://doi.org/10.1130/G40207.1.

Numerical Modeling Methodology

Stokes flow and temperature advection-diffusion were numerically calculated in 2D using Underworld (Moresi et al. 2007), a particle-in-cell finite-element code. The Stokes flow calculation assumes incompressibility and uses the Boussinesq and plane strain approximations. Material density and viscosity are stored on approximately 12 particles per element and are used as Gaussian quadrature points. Linear shape functions are used. The mesh is Cartesian with a 3:1 and 256 x 768 width to height ratio and resolution respectively. The model depth is 2900km and the resolution is vertically refined to double the resolution in the upper 580 km.

Mantle convection is driven purely by uniform internal heating. The temperature (T) of the top wall is set to $T = 0$ and all other walls are insulating. The thermal diffusivity κ is uniform everywhere. The viscosity at the highest mantle temperature is chosen to calculate the representative viscosity (η_0). The Rayleigh Number is calculated as:

$$Ra = \frac{\alpha g \rho_0 H L^5}{\kappa \eta_0 c} \qquad \text{(S1)}$$

where α is the thermal expanisivty, g gravity, ρ_0 the density at the highest mantle temperature, H is the internal heating measured in Wkg^{-1}, L the thickness of the entire mantle and c the specific heat. The model is set such that the Rayleigh number prior to the lid breaking event is $Ra = 10^9$, which marginally declines as the mantle cools.

Stress and time are non-dimensionalized using the scalings Eq. S2 and S3, where $\Delta\rho$ is the largest density contrast in the system driving flow. Distance z is non-dimensionalized as $z' = z/L$.

$$\sigma' = \frac{\sigma}{\Delta\rho g L} \qquad \text{(S2)}$$

$$t' = t\,\frac{\Delta\rho g L}{\eta} \qquad \text{(S3)}$$

The heat-pipe process is approximated by limiting the geotherm to a chosen solidus. This represents the heat buffering effect of melt generation and effective transport to the surface where the melt is effectively instantaneously cooled. Moore and Webb (2013) showed that transport of melt to the surface has the effect of introducing a downward advective term, which produces a geotherm which is colder than steady-state. Rozel et al. (2017) showed that if the melt instead resides in the crust, the resulting geotherm is warmer than steady-state. For simplification, these two processes are approximately averaged by assuming there is no downward advection and no crustal magmatic heat-sources.

We are primarily interested in the switch from the heat-pipe mode to mobile lid convection. In the heat-pipe model, this switch occurs when melting has mostly switched off (Moore and Webb, 2013). Therefore the first purpose of the solidus implementation is to trigger the mantle regime switch. The second purpose is to generate the heat-pipe geotherm, which is colder than the typical stagnant lid model. The lithospheric thickening model is not significantly dependent on the solidus implementation, as tested by running a traditional stagnant-lid model, triggering the switch by arbitrarily lowering the yield stress.

The solidus temperature depends on depth z and is chosen as $T_s = 720 + 2.0\ z\ °C$. This choice results in the steady-state geotherm being close to the solidus and allows melting to eventually switch off with exponentially declining heat-production. This choice is arbitrary and reproduces the heat-pipe mechanism described by Moore and Webb (2013) and Kankanamge and Moore (2016), in a simple manner. While this solidus allows melting to occur when a lid is present, it results in unrealistically deep melting in the mobile lid mode. This is likely to represent a difference in composition and melt depletion between the stagnant lid lithosphere and the mobile lid asthenosphere. Our models switch to a relatively shallow solidus of $T_s = 1200 + 3.9\ z\ °C$ once the lid recycling event begins, which is a smooth transition as melting has previously switched off at this point. Comparisons of models with and without this solidus switch show no difference in craton stability or stress evolution, indicating that it is not an important factor for the cratonization process.

There are two 'materials' in the models: one which represents the typical mantle material (mantle material) and one which represents chemically differentiated material approximating both felsic crust and depleted lithospheric mantle (continental material). Particles in the upper 72.5 km of the model domain are initially set as continental material and everything below mantle material.

The two materials have different viscosity and density functions. Both have a viscosity which is temperature and stress dependent (eq. S4). For simplicity, mantle phase transitions are ignored. Temperature dependence follows the Frank-Kamenetskii approximation of the Arrhenius formulation, with $E = 5$, such that the largest viscosity contrast is 5 orders of magnitude. Stress is calculated using the second invariant of the strain-rate tensor, $\dot{\epsilon}_{II}$. The viscosity is calculated iteratively and if its stress rises above a yield stress τ_y, an effective viscosity is calculated that limits the stress to the yield stress, following Moresi and Solomatov (1998).

$$\eta(T, \dot{\epsilon_{II}}) = \min(\eta_0 e^{-\frac{E(T-T_0)}{\Delta T}}, \frac{\tau_y}{\dot{\epsilon}_{II}}) \qquad \text{(S4)}$$

The reference temperature T_0 is chosen as the highest temperature of the initial steady-state stagnant lid / heat-pipe model. The mantle reference viscosity (η_0) at this temperature is chosen to set Ra. The $\eta_0$of the continental material is chosen to be the same as the mantle, as it already high as a result of its low initial temperature. The yield stress depends on depth (z in km), which represents a pressure dependence:

$$\tau_y = \mu z \qquad \text{(S5)}$$

$\mu = 0.05$ and 0.47 for the mantle and continental materials respectively. These can be dimensionalised as $\mu = 0.064$ and $0.6\ MPa/km$, assuming that $\Delta\rho = 130\ kg\ m^{-3}$. This pressure dependence captures the high plastic strength of thickened cratonic lithosphere and represents the minimum strength of all operating deformation mechanisms at high pressure. The high μ for the continental material is likely to be the result of its high melt depletion (Karato, 2010) and cold temperature.

The density of all materials varies linearly with temperature:

$$\rho(T) = \rho_0(1 - \alpha(T - T_0)) \qquad \text{(S6)}$$

The reference density ρ_0 and thermal expansivity of the mantle material are chosen to set Ra. The continental material has a smaller ρ_0 than the mantle material, in order to control its relative buoyancy compared to mantle downwellings. Following Cooper et al. (2006), this relative buoyancy is defined as:

$$B = \frac{\rho_0 - \rho_c}{\rho_0 \alpha \Delta T} \quad \text{(S7)}$$

where ρ_0 and ρ_c are the reference densities for the mantle and continental materials respectively. For the models shown, this is set as $B = 0.36$. Assuming that $\rho_0 \alpha \Delta T \approx 130\ kg\ m^{-3}$, this gives a lithospheric density which is on average $47\ kg\ m^{-3}$ less dense than the mantle, if slab buoyancy stresses have not changed significantly over time. If buoyancy stress has scaled proportionally with temperature, a temperature decline of $200^o C$ gives a cratonic lithosphere density of $41\ kg\ m^{-3}$ less dense than the mantle.

These choices of μ and B for the continental material result in thickening and stabilization of the cratonic lithosphere at approximately 300 km thickness. Increasing μ or B will result in thinner stabilized lithosphere (Cooper et al. 2006). Additionally, a smaller B can be compensated for by a larger μ and vice-versa.

Time Scaling

The chosen model Ra is likely to be smaller than the actual value for the Earth ~3Ga. Ra is a ratio of a flow time-scale to a thermal diffusion time-scale. For scaling purposes, we assume that the model flow time-scale (Eq. S3) is accurate and thermal diffusion is over-estimated.

We assume that for the modern Earth, $\Delta\rho \approx 130\ kg\ m^{-3}$ and $\eta \approx 10^{22} Pa\ s$ (taking the lower mantle viscosity). These values should differ for a hotter Earth. The mantle viscosity varies from a reference value, η_0, with temperature according to:

$$\eta(\delta T) = \eta_0 e^{-E\delta T/\Delta T} \quad \text{(S8)}$$

where δT is the temperature increase from the reference value and ΔT is the temperature contrast between the Earth's surface and the mantle interior. A temperature increase of 200℃ lowers this viscosity to $\eta_0 \sim 10^{21} Pa\ s$, for $E = 13$. A hotter mantle has a lower density, however the oceanic crust is more buoyant as a result of increased melting. It is assumed that these factors are similar so that $\Delta\rho$ is equivalent to the modern Earth. A 200℃ mantle temperature increase is then estimated to reduce the convective time-scale to 10% of the modern Earth.

Individual cratonization events then typically take about 10Ma and complete thickening takes about 80Ma.

Stress Measurement and Scaling

Three cratonic nuclei form in the models (left, center and right in Fig. 2) and stress is measured separately for each. Stress is measured as $\sigma = 2\eta\dot{\epsilon}_{II}$ and peak stress is taken as the 95th percentile of σ for a given nuclei at a particular time. This choice eliminates the erroneous measurement of maximum stress on particles which have been removed and entrained by mantle flow.

Figure S1 shows the evolution of the maximum craton stress state through time, for a 400 Ma period including the lid breaking event. The data for the left cratonic nucleus is used for Fig. 1.

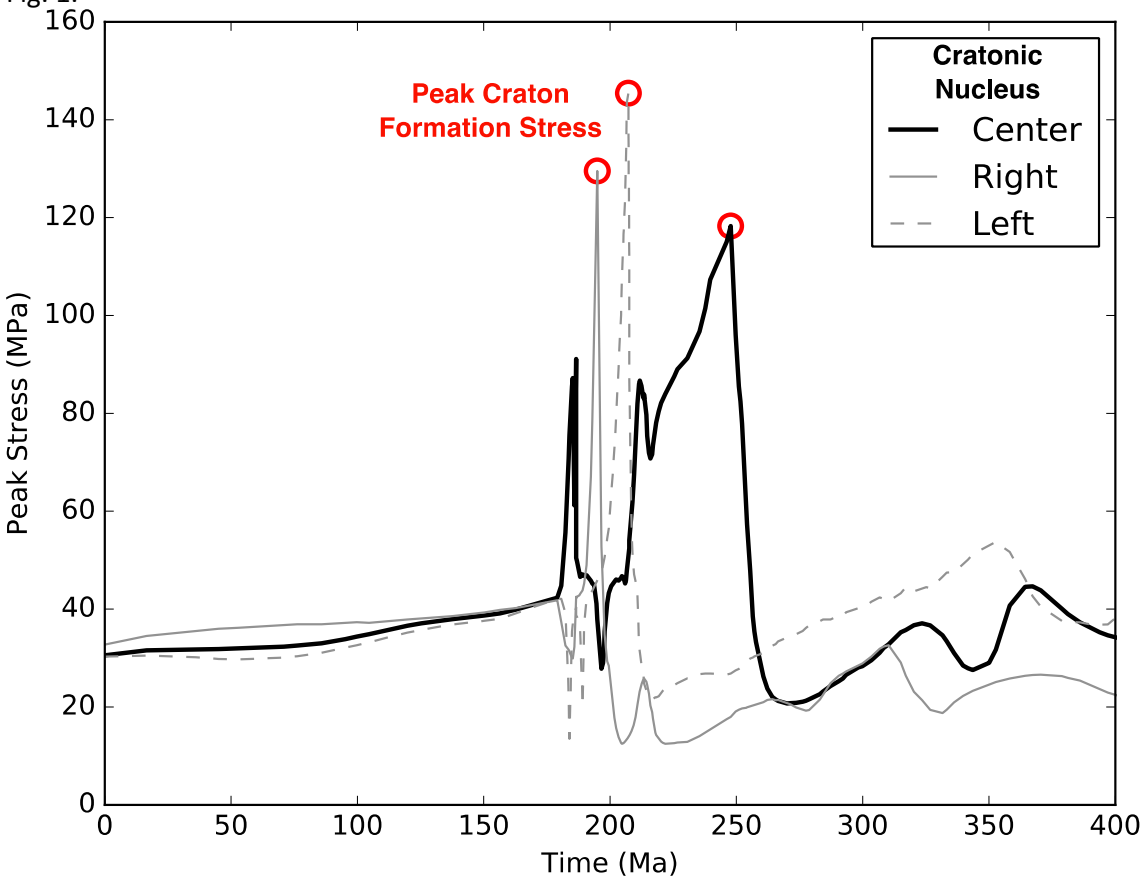

Figure S1) Peak stress measured individually for the three cratonic nuclei, taken from model shown in Figs. 1 (center panel) and 2.

This gives a peak stress of about 30 MPa during the stagnant lid and mobile lid regimes. During the lid breaking event, the maximum stress is 150 MPa. This scaling is for illustrative purposes; for the study it is the relative stress between the stress pulse and the mobile lid immediately after which is important. The Archean mobile lid stress state is scaled by calculating the Ra decrease corresponding to $200^{o}C$ of cooling, assuming Eq. S8.

The crustal thickness data of Dhuime et al. (2015) is also used to estimate stress variation over time. We assume that the density of juvenile crust has not changed significantly and that it in isostatic equilibrium, with its thickness varying proportional to the compressive crustal stress state. A current crustal thickness of 30 km is assumed.

Model Resolution

The heat-pipe model begins with $\mathrm{Ra} = 10^{9}$, which reduces to $\mathrm{Ra} = 5 \times 10^{8}$ at the time of lid collapse, as a result of radiogenic decay. Comparisons of 2D convection in a box with a temperature-dependent viscosity modelled without particles in Underworld, have been

compared to convection benchmarks (Blankenbach et al., 1989) and are described at: https://github.com/underworldcode/underworld2/blob/master/docs/examples/1_04_BlankenbachBenchmark_Case2a.ipynb.

A resolution of 128x128 reproduces the benchmark within 4% error, for $Ra = 10^7$. The boundary layer thickness scales proportionally to $Ra^{-\frac{1}{3}}$, and so our higher Ra corresponds to a reduction in boundary layer thickness by a factor of 3.7. Our model mesh is 4 times finer in the upper mantle and therefore is sufficient to produce similar results for our higher Rayleigh number. Our models have a vertical resolution of 512 in the upper 660km of the model and include particles, so the thinner boundary layer formed in the mobile lid regime is sufficiently captured. Our primary interest in the mobile lid regime models is the convective stress on the cratons, for which the 6km spacing is sufficient for capturing the buoyancy forces of the unstable part of the boundary layer, which is typically ~70km thick.

Damage Model

For the stagnant lid to break, its yield strength needs to be limited to 10-50MPa. Rozel (2012) showed that this low strength can result from dynamic weakening by grain-size reduction and a switch to diffusion creep. We assumed for our simplified models that this weakening had already occurred. Here we demonstrate with a short model that a damage accumulation model with dynamic weakening can reproduce our craton formation model, justifying our simplification.

The model below begins with a 72.5 km harzburgite layer and an embedded 12 km thick continental crust, with densities of 2900 and 3269 $k\mathrm{g}/\mathrm{m}^3$ respectively. Eclogite formed during previous crust formation is assumed to have recycled through the thin heat-pipe lid. A finite plastic strength following the Von Mises criterion is set to 2.94 MPa/km, representing crust with existing faults and limited at 100 MPa. Materials incur strain and temperature dependent damage, representing reduction and growth of olivine grain-size (following Rozel, 2012), which can reduce the yield limit by 90% (mantle) and 50% (continental crust and lithosphere) and allow the lid to break. The pressure-dependence of olivine (Karato, 2010) is modeled as a 1 Mpa/km increase in yield strength below 72.5 km (0.1 MPa/km for mantle), giving thickened lithosphere a strength of 300 Mpa. A 12km thick layer, with a yield stress one order of magnitude lower than the mantle, forms above new mobile lid ocean floor and allows subduction to occur.

The damage parameter is tracked on each particle. It increases with integrated strain and decreases according to an Arrhenius healing function, with an activation energy of 287 kJ/mol, which is conservative (Rozel, 2012). Though strain-rates are small in the cold, viscous upper parts of the stagnant lid, healing is also relatively slow and damage can accumulate after a number of mantle overturns (Fig S2). Though the damaged lithosphere has a decreased yield strength, it does not fail immediately, but requires the same development of an increased stagnant lid slope which developed in the simplified models for the lid-breaking event to initiate.

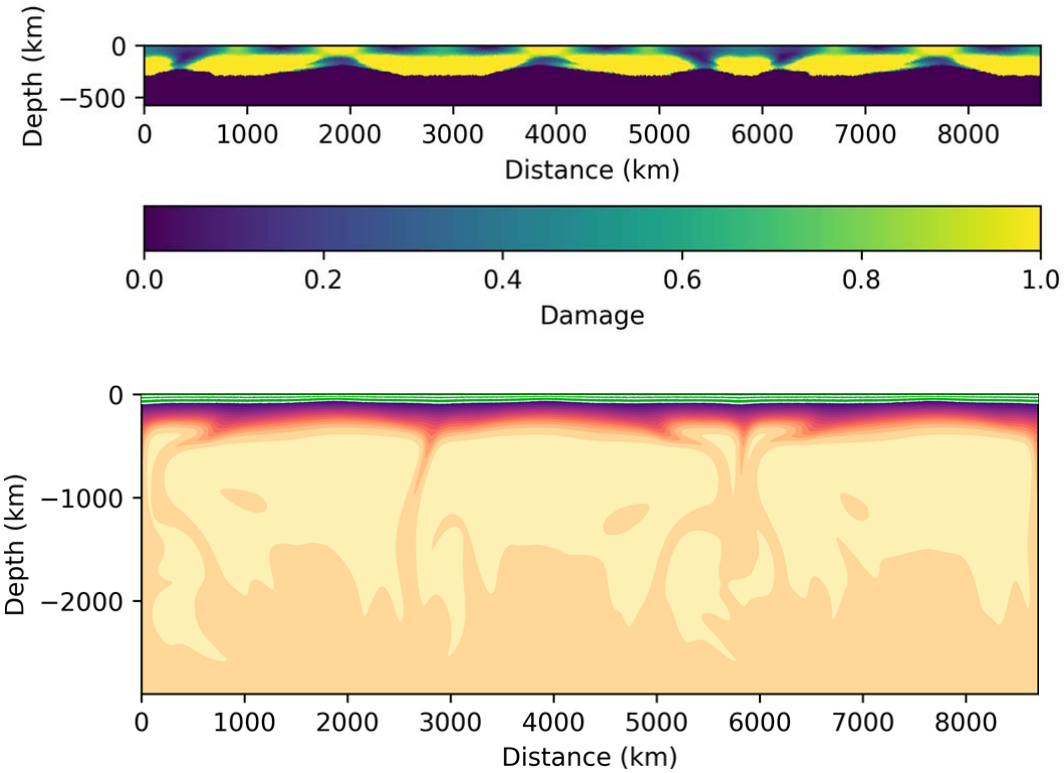

Figure S2) Steady-state damage (above) during stagnant lid convection, prior to stagnant lid collapse (below)

A)

B)

C)

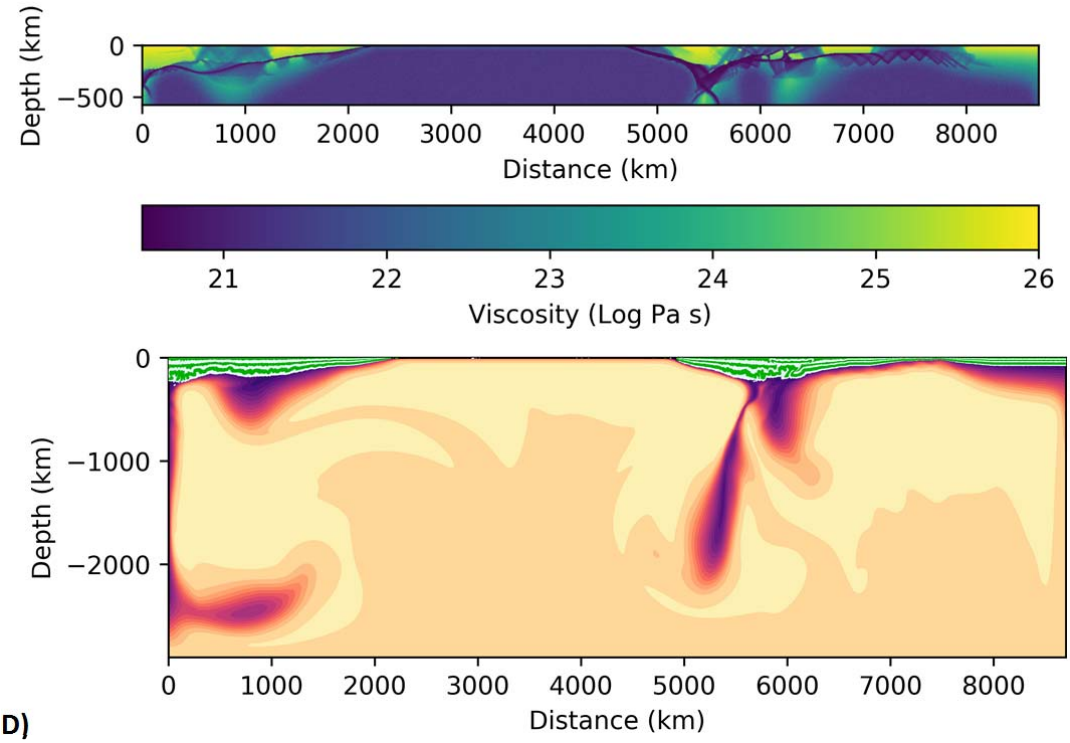

D)

Figure S3) Evolution of lithospheric viscosity. The convective stresses have risen to magnitudes similar to the lid yield strength (A), eventually leading to lid failure (B) and the formation and stabilization of cratonic lithosphere (C,D).

The lid-breaking event is shown in the evolving viscosity plot of Fig S3. Failure is more localized, compared to the simplified models, as a result of the hetereogeneity of damage at the base of the depleted lithospheric layer. The lid breaks in the same regions however, where the lid is initially thinned and thickened and therefore higher stresses are located. Once the lid-breaking event initiates, each lateral section of the depleted layer fails and thickens, under the influence of the mantle downwellings, regardless of initial weakening. Stabilization occurs in the same way as the simpler models, with an increase in yield strength at high pressure switching off failure upon thickening.

Movie

A movie is also included in the data repository, which shows a typical model evolution. The model is designed to demonstrate the craton formation process and the subsequent stability during multiple mantle overturns and craton migration.

References

Cooper, C.M., Lenardic, A., Levander, A. and Moresi, L., 2006. Creation and preservation of cratonic lithosphere: seismic constraints and geodynamic models. Archean Geodynamics and Environments, pp.75-88.

Dhuime, B., Wuestefeld, A. and Hawkesworth, C.J., 2015. Emergence of modern continental crust about 3 billion years ago. Nature Geoscience, 8(7), pp.552-555.

Kankanamge, D.G. and Moore, W.B., 2016. Heat transport in the Hadean mantle: From heat pipes to plates. Geophysical Research Letters, 43(7), pp.3208-3214.

Karato, S.I., 2010. Rheology of the deep upper mantle and its implications for the preservation of the continental roots: A review. Tectonophysics, 481(1), pp.82-98.

Moore, W.B. and Webb, A.A.G., 2013. Heat-pipe earth. Nature, 501(7468), p.501.

Moresi, L. and Solomatov, V., 1998. Mantle convection with a brittle lithosphere: thoughts on the global tectonic styles of the Earth and Venus. Geophysical Journal International, 133(3), pp.669-682.

Rozel, A., 2012. Impact of grain size on the convection of terrestrial planets. Geochemistry, Geophysics, Geosystems, 13(10).

Rozel, A.B., Golabek, G.J., Jain, C., Tackley, P.J. and Gerya, T., 2017. Continental crust formation on early Earth controlled by intrusive magmatism. Nature, 545(7654), pp.332-335.